



HAL
open science

On-line determination of aggregate size and morphology in suspensions

Michel Cournil, Frédéric Gruy, Patrick Cugniet

► **To cite this version:**

Michel Cournil, Frédéric Gruy, Patrick Cugniet. On-line determination of aggregate size and morphology in suspensions. 9e congrès de la SFGP. "Du rayonnement scientifique à la diffusion des technologies", Sep 2003, Saint-Nazaire, France. C2-9 pp. 71-78. hal-00839630

HAL Id: hal-00839630

<https://hal.science/hal-00839630v1>

Submitted on 27 Sep 2013

HAL is a multi-disciplinary open access archive for the deposit and dissemination of scientific research documents, whether they are published or not. The documents may come from teaching and research institutions in France or abroad, or from public or private research centers.

L'archive ouverte pluridisciplinaire **HAL**, est destinée au dépôt et à la diffusion de documents scientifiques de niveau recherche, publiés ou non, émanant des établissements d'enseignement et de recherche français ou étrangers, des laboratoires publics ou privés.

ON-LINE DETERMINATION OF AGGREGATE SIZE AND MORPHOLOGY IN SUSPENSIONS

Michel Cournil, Frédéric Gruy and Patrick Cugniet

Ecole des Mines de Saint-Etienne, Dept SPIN, URA CNRS 2021
158, Cours Fauriel, 42023 Saint-Etienne Cedex 2 (France)

Abstract. Information about the aggregation state of fine particles is an important element for process control, product quality monitoring and fundamental understanding in many cases of industrial slurries. When aggregates are small or fragile objects, their withdrawal is difficult and off-line characterization may be a source of error. This work deals with the application of different in line methods to the characterization of silica aggregate size and morphology. These methods are based on turbidimetry. One of them consists of the analysis of the turbidity fluctuations and is operated on a commercial instrument. The other one uses the aggregate settling velocity which is determined by turbidimetry too, however with a home-made apparatus. This work gives us the opportunity to define morphological models for small aggregates and to calculate their drag coefficient. Thanks to these models, the aggregate morphological characteristics and the number of their constituting particles can be derived from the experimental results. Agreement between the different methods is examined and discussed.

INTRODUCTION

Contrary to agglomerates which are commonly cemented by crystalline bridges which confer them a rigid and solid structure, aggregates are most of the time small and fragile objects. In particular, in most experiments, their size does not exceed a maximum value which results either from the dynamic balance between aggregation and fragmentation or from zero aggregation efficiency beyond a certain size [1-2]. For fundamental reasons as well as for process monitoring purpose, real time knowledge of the aggregate size and morphology may be very useful. For these determinations, both on-line and in-line methods can be envisaged. Off-line methods, however, do not ensure isokinetic withdrawal, particularly, for small particles, and may damage fragile aggregates. In situ techniques would be certainly ideal; however, only very few exist and they need to be validated. Turbidimetry has been proved to be a particularly efficient method for in situ particle size measurements [3], particularly in aggregating systems [1]. Turbidimetry is based on light scattering by suspensions and rests on the Mie theory [4]. However, the scattering properties of small aggregates of micronic particles, for instance, is not completely known and requires additional research. Since the works of Tessely et al. [5], analysis of turbidity fluctuations has been shown as particularly interesting for the determination of particle number and size; this principle has given rise to a commercial instrument (Aello 4000).

The present work is devoted to the characterization of aggregates of silica formed in a stirred vessel. Aggregation itself has been studied by in situ turbidimetry [6-7]. Final aggregates are characterized both using turbidity fluctuations and settling velocity measurements. Interpretation of these data requires preliminary theoretical tasks: morphological modelling of the aggregates and calculation of their light scattering section and drag coefficient. Comparison between the morphology and size respectively given by each method is presented and commented on.

EXPERIMENTAL PART

1. Materials techniques and procedure

Aggregation experiments are performed on samples of monodisperse silica spheres (1.5 μm in diameter, *Geltech Inc* products). Aggregation is studied in water at pH values 2 to 4.

The reactor used for this study of aggregation is a stirred tank the diameter of which is 120 mm (Figure 1). This reactor is equipped with four baffles. Liquid depth in the vessel is equal to diameter. Bottom part of the tank is rounded. Agitation is ensured by a four-bladed 45° Teflon impeller of diameter 60 mm. Temperature is kept constant at 25.00 °C ± 0.01 °C by a double-jacket. The reactor is fitted with an optical system to measure in situ the suspension turbidity in the wavelength range 350 nm-800 nm. Details can be found in [6].

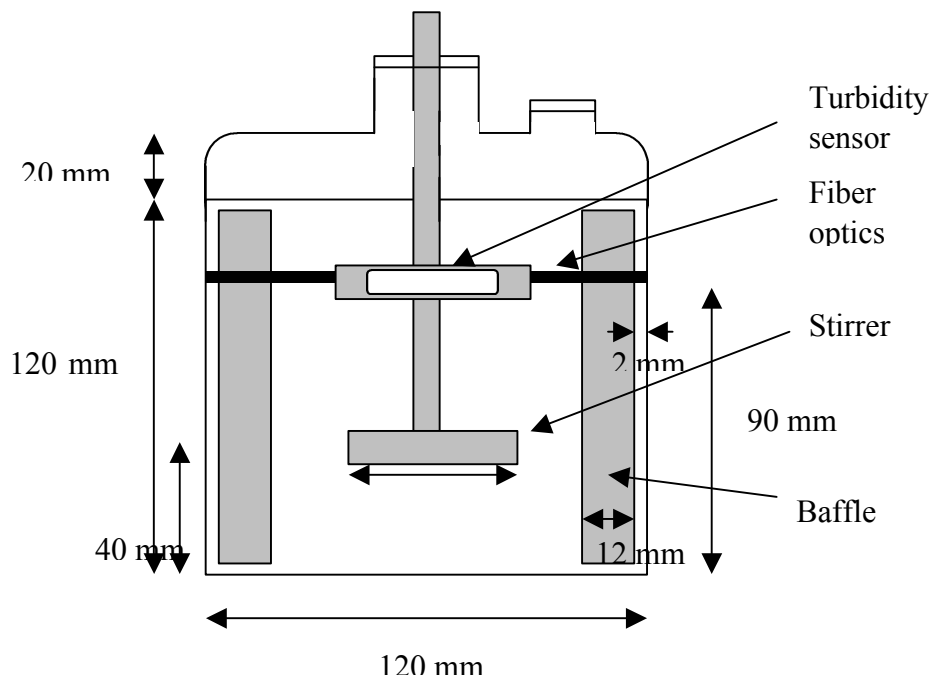


Figure 1. Schematic representation of the aggregation reactor

Turbidity τ expresses the extinction phenomenon of an incident light beam due to light scattering by solid particles; it is defined by relation:

$$\tau(\lambda_0) = \frac{1}{L_{opt}} \ln \frac{I_0(\lambda_0)}{I(\lambda_0)} \quad (1)$$

in which λ_0 is the wavelength, $I_0(\lambda_0)$ the intensity of the incident beam and $I(\lambda_0)$ the intensity of the transmitted beam after an optical path of length L_{opt} .

Turbidity depends on the mean diameter d_p particle density function f according to the integral:

$$\tau(\lambda_0) = \int_0^\infty C_{ext}(d_p) f(d_p) dd_p \quad (2)$$

Particle extinction section C_{ext} is derived from the Mie theory [4]; its calculation is relatively easy for spherical, compact, or large particles, however much more delicate for small, non compact aggregates [8]. From equation (2), it appears that variations in the particle density function f result in turbidity variation. For instance, in the case of 1.5 μ m silica particles in water, turbidity decreases with aggregation, whereas it increases in the case of 0.5 μ m particles. When particles leave the measurement cell, due to settling for instance, turbidity decreases obviously. These characteristics will be exploited later on.

Aello 4000 measurement cell is external to the reactor and located on a by-recirculation loop; thus measurements are in line and not in situ as previously. This apparatus delivers the turbidity signal of the suspension located in its measurement cell, however with a special interest in the signal fluctuations around its mean value. From these data, two parameters are calculated, mean extinction section C_{ext} and particle number in the cell n . Compared to our in situ determinations, this measurement procedure is liable to damage the aggregates, however this effect is certainly reduced because shear stress in the loop is considerably lower than in the reactor and pumping conditions are relatively smooth. This is confirmed by the identical turbidity levels observed in the two experimental systems.

Aggregation of a 0.246 g silica sample is performed in the previous reactor at given stirring rate. Whatever the experimental conditions, turbidity reaches a constant value after a few tens of minutes at the maximum; this plateau is generally interpreted as a steady state of the aggregate size distribution in the system and is characterized by a maximum aggregate size. After two hours, this means during this steady state, agitation is stopped; particle settling is clearly observed and turbidity decrease is recorded. In similar experiments, suspension is pumped to the Aello 4000 cell and characterized during the aggregation process and at its end.

2. Principle of interpretation of the sedimentation experiments

The turbidity probe is vertically located at the two-thirds of the vessel radius halfway between two baffles, and mounted at 4.8 cm from the upper surface of the liquid (Figure 2)

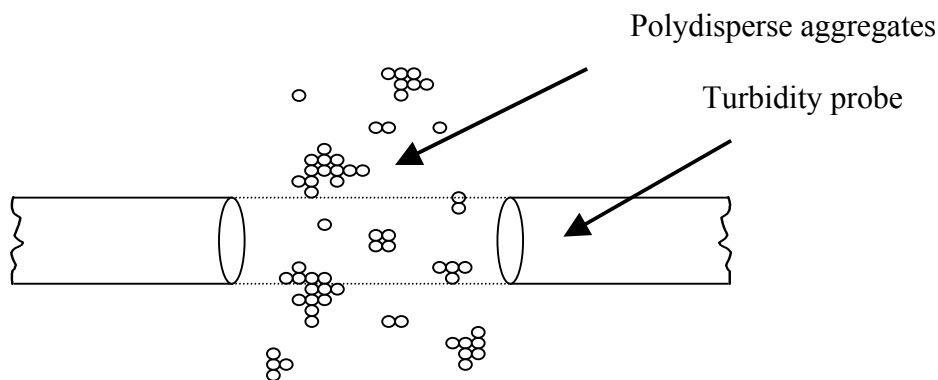


Figure 2. Aggregate settling as detected by the turbidity sensor

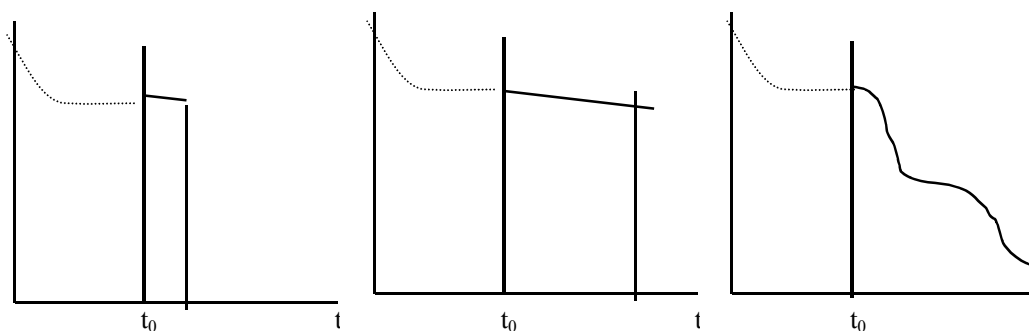


Figure 3. Turbidity variation during aggregate sedimentation, : a: large monodisperse aggregates; b: small monodisperse aggregates; c: polydisperse aggregates.

As soon as agitation is stopped, aggregates start settling and gradual decrease in turbidity is observed. In the ideal case of monodisperse aggregates, the turbidity signal keeps constant for a while and sharply decreases only when the aggregates initially located near the liquid

surface have crossed the measurement window. In the case of polydisperse aggregates, settling results in a classification of the aggregates according to their size and turbidity drop is not as sharp. Thus, according to the aggregate population nature, different turbidity plots against time are observed.

In Figure 3 we have represented the initial turbidity decrease due to aggregation in the stirred vessel in the time interval $[0, t_0 = 2 \text{ hours}]$ then the turbidity decrease due to sedimentation. Cases a and b are relative to monodisperse aggregates; case c, which concerns polydisperse aggregates, is the most commonly observed.

Settling velocity of a silica spherical particle in water is given by Stokes law :

$$v_1 = \frac{2}{9} \rho \frac{a_1 g}{\mu} \quad (3)$$

in which a_1 is the sphere radius, g , the gravity, μ , the liquid dynamic viscosity and ρ the density difference between silica and water.

In the case of fractal-like aggregates, previous relation becomes:

$$v = v_1 \frac{i}{\beta} \quad (4)$$

with:

$$\beta = \frac{a_i}{a_1} = \frac{i}{S} \Omega^{1/D_f} \quad (5)$$

in which i is the number of primary particles in the aggregate, Ω a corrective drag coefficient, a_i , the aggregate outer radius, v , its settling velocity. D_f , the aggregate fractal dimension, is defined by this relation. S , *structure factor*, depends on D_f and is obtained from simulations. In turbulent aggregation, D_f is most of the time equal to 2.4 and $S = 0.79$ [8].

From experimental curves similar to plots of Figure 3a and 3b, we can easily calculate v by dividing the sensor mean depth from the top of the liquid (here 4.8 cm) by the settling duration. Then a_1 is deduced from Eqn 3. This has been done for silica particles in conditions of non aggregation (pH = 8) and good agreement has been found. For experimental plots similar to Figure 3c, we have to choose a characteristic settling time to be able to determine the aggregate size. This will be discussed further.

3 Experimental results

3.1 Determination of the corrective drag coefficient

As no model was available to determine drag coefficient Ω particularly for small aggregates, we performed specific experiments. In order to use handy objects, we did experiments on 1 mm glass beads aggregates that we prepared ourselves [6]. Different sizes (2 to 80 particles) and morphologies were obtained so. To keep Stokes settling conditions, we studied sedimentation in glycerol. Sedimentation time, which is relatively long, as determined by direct observation of the settling objects, thus settling velocity was easily obtained. To apply Eqns 4 and 5, we needed to know a_i . We took it equal to the radius of the sphere which had the same projected area as the aggregate. As the aggregates were not necessarily isotropic, we obtained their projected surface area either from standard image analysis procedures of their photograph, or by direct calculation on the geometrical objects, knowing the coordinates of the primary particles. Then Ω could be derived from Eqn 4. In all cases, Ω was found practically equal to 1 (with the specified choice of a_i).

3.2 Settling of 1.5 μm silica particles

Using procedure described in section 2, we obtain the turbidity variation shown in Figure 4. Agitation was interrupted in the reactor after t_0 hours aggregation. Plots of Figure 4 have the same shape as plot of Figure 3c. As aforesaid in section 2, characteristic time of settling should be chosen. Taken into account the existence of a main sedimentation wave on the different plots of Figure 4 we chose characteristic times corresponding to the end of this wave.

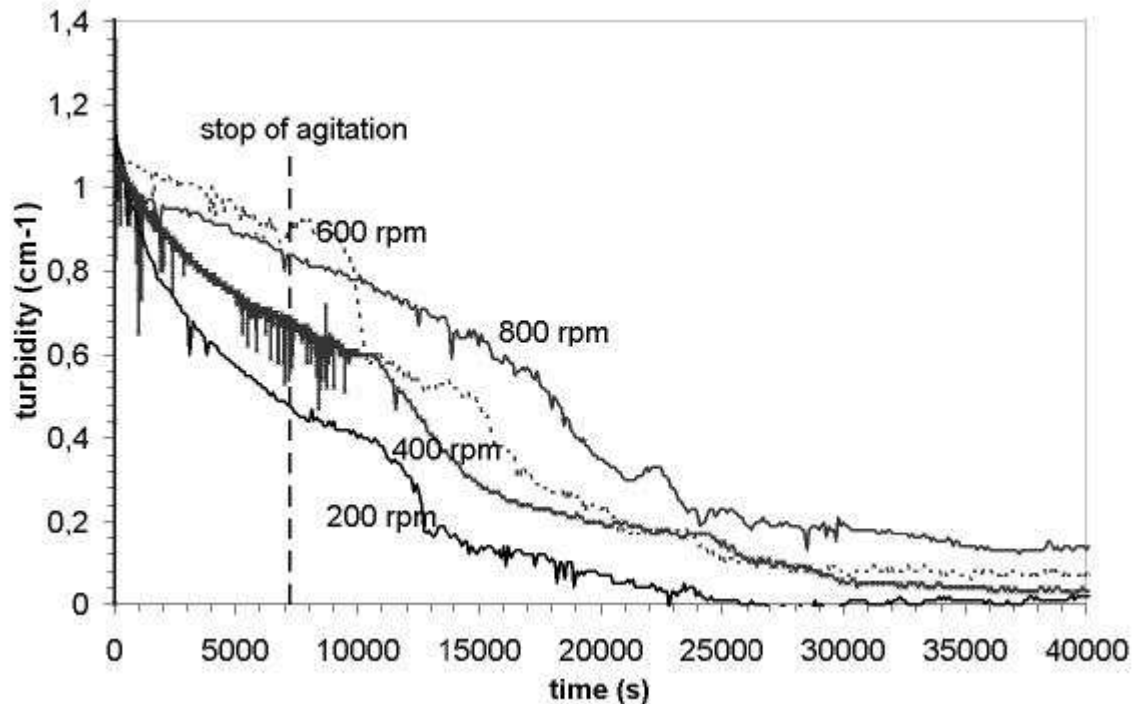


Figure 4: Settling of 1.5 μm silica in water ($\text{pH} = 3$, $\lambda = 550 \text{ nm}$)

Table 1 shows the different settling times and normalized settling velocity v/v_1 obtained for different stirring rates.

Table 1: Normalized experimental settling velocity of silica aggregates formed at different stirring rates

Stirring rate (rpm)	Settling time(s)	v/v_1
200	6000	5.8
400	8000	4.4
600	13000	2.7
800	15400	2.3

3.3. Aello 4000 determinations

As aforesaid, the Aello 4000 equipment allowed us to obtain C_{ext} and number n of particles in the cell at any time, in particular, total number of silica particles n_0 is known. This is the initial number of particles which is measured at time zero prior to aggregation. Dividing n_0 by n

gives us L the mean number of silica particles per aggregate. Data relative to the aggregation-fragmentation steady state are reported in Table 2 for different stirring rates.

3.4. Image analysis

Attempts of aggregate removal after 2 hours aggregation have been made. After their withdrawal with a pipette, the samples have been carefully dried, then observed with a microscope coupled with an image analyser (Zeiss Axioskop microscope, magnification : x 500; video camera J C KY-F58; Leica - in software). Photographs of the removed samples have been processed in order to determine the number of primary particles per aggregate. Results are reported in Table 2.

Table 2: Estimation of the mean number of silica particles per aggregate

Stirring rate (rpm)	200	400	600	800
C_{ext} (m ²)	23	14	6	5
n	210	400	1000	1500
n_0/n (L)	28	15	6	4
Particle number (from image analysis)	46	...	25	20
Particle number (from settling data)	20	15	5	5

Table 3: Calculated values of normalized (v/v_1) settling velocity of aggregates for different fractal dimensions and particle numbers

Particle number	Fractal dimension D_f							
	2	2.2	2.3	2.4	2.5	2.6	2.7	2.9
8	3.1	3.2	3.2	3.3	3.4	3.6	3.7	3.9
16	4.3	4.6	4.8	5.0	5.2	5.4	5.7	6.2
24	5.3	5.7	6.0	6.3	6.6	7.0	7.3	8.0
32	6.0	6.6	7.0	7.5	7.9	8.3	8.8	9.7

DISCUSSION

1. Settling velocity calculations

Using Equations (3) to (5) of section 2 and experimental determinations of the corrective drag coefficient (section 3.1), we can predict the normalized settling velocity of aggregates of given number of primary particles and given fractal dimension. These calculations are reported in Table 3

Now this table can be used as follows:

- i) the respective experimental normalized settling velocities of the aggregates formed at different stirring rates are extracted from Table 1;
- ii) the respective closest values of normalized settling velocity are searched for in the columns $D_f = 2.4 - 2.5$ which is the likely fractal dimension of the aggregates. In fact, the fractal dimension could have been obtained by image analysis of experimental samples, however, only in the case of very large aggregates of small particles. This is not the case here. Thus, we selected the present values because they were commonly found from previous experiments and simulations.
- iii) the corresponding particle number in the aggregate is found after interpolation on data of Table 3 and then reported in last row of Table 2.

We can now compare the estimations of particle number in small silica aggregates which were derived using the different methods.

- i) Aello 4000 measurements and determinations from settling velocities are in good agreement and indicate that this particle number is very low. Aello equipment is supposed to give reliable results for particles ranging between 1 and 250 micrometers in equivalent diameter;
- ii) direct measurements on withdrawn samples are very different and certainly non representative. They confirm the well known difficulty of isokinetic removal of small objects. Similar studies were performed on 0.5 μ m silica particles and lead us to the same conclusions [6]. The Aello 4000 apparatus still provided us with correct results in spite of the low value of the particle diameter.

2. Maximum aggregate size

As we mentioned in the introduction of this paper, the existence of maximum aggregate size can be due to two main reasons: fragmentation or collision efficiency becoming zero beyond a critical size.

2.1. Fragmentation

The occurrence of breakage depends on the balance between the disaggregation effects due to the action of the fluid and the overall cohesion of the aggregate due to the interactions between primary particles. The hydrodynamic effects are of different nature according that the aggregate is larger or smaller than the Kolmogorov microscale. Only the latter case is compatible with the experimental conditions of this study. It corresponds to a shear stress

originating from the local velocity gradient $\dot{\gamma}$ and acting on the aggregate. The breakage rate

or the fragmentation kernel K_f is generally assumed to be proportional to $\dot{\gamma} e^{-\frac{\sigma}{\tau_s}}$, where σ is the mean mechanical strength of the aggregate and τ_s is the mean shear stress. Thus, the breakage

rate depends on the hydrodynamic conditions of the flow, via $\dot{\gamma}$ and on the characteristics of the aggregates: outer radius, fractal dimension, primary particle radius and cohesion force between two primary particles (typically van der Waals force).

In recent works [2, 7-8] on aggregation of titanium dioxide or silica in similar conditions, however, we came to the conclusion that such fragmentation kernels were not able to interpret the maximum size observed in our experiments, thus we adopted the following theoretical approach.

2.2. Zero collision efficiency

This approach was especially developed by Brakalov [9]. It is known that the collision efficiency between two equally sized spherical particles decreases with the particle size. The decrease is sharper as the particles (aggregates) are porous. Otherwise, the aggregate, which

results from too smaller aggregates, can be too loose to survive. Brakalov shows that it exists a maximum value for the aggregate size. From different experimental works, it appears that the maximum particle size a_L depends on shear rate, according to relation:

$$\frac{a_L}{a_1} = \dot{\gamma}^{-c'} \quad (6)$$

In recent works on aggregation in the same reactor [2, 6, 7], we found values from 0.22 to 0.60 for exponent c' . Moreover, after integrating the assumption of zero aggregation efficiency beyond this size in our models, we obtained good agreement between predicted and observed dynamics.

We recall that the gradient velocity as a function of the turbulent energy dissipation rate ϵ_m and kinematic viscosity ν :

$$\dot{\gamma} = \frac{\epsilon_m}{\nu}^{\frac{1}{2}} \quad (7)$$

Mean value of ϵ_m is given by the well-known equation:

$$\bar{\epsilon}_m = \frac{N_p \omega^3 D_s^5}{V} \quad (8)$$

in which, N_p is the power number, D_s the stirrer diameter, ω the rotation rate of the stirrer and V the volume of the suspension..

Using the results of the present study (respectively Aello measurements and settling data from Table 2) and equations (5-8), we can now verify relation (6) in our case and determine exponent c' . Good agreement is found, which validates the mathematical form of Equation (6) and respective values of c' are: 0.24 and 0.19. These values are of the same order of magnitude as previous results obtained on titanium dioxide aggregation [2].

CONCLUSION

This study clearly proves the interest of in situ or in line particle size determinations, especially based on turbidimetry, for aggregate or agglomerate characterization. Thanks to this procedure, small and fragile objects can be characterized in situ without taking the risk of damaging or non isokinetic methods. Another interesting aspect of the Aello 4000 measurements is the possibility of quasi-instantaneous characterizations, allowing in this to characterize rapidly changing media or objects. From a fundamental point of view, this work has allowed us to model the settling velocity of small ramified objects, which was not known so far. The dependence on the aggregate particle number has been determined according to the stirring rate. Thanks to these data progress can be expected in the understanding of the aggregate fragmentation mechanisms.

REFERENCES

- [1] Saint-Raymond, H., Gruy F., Cournil M., J. Colloid and Interf. Sci., 202 (1998), 238.
- [2] Tontrup C., Gruy F., Cournil M., J. Coll. Inter. Sci., 229 (2000), 511-525.
- [3] Crayley G.M., Cournil M., Di Benedetto D., Powder Technol. 91 (1997), 197.
- [4] van de Hulst H.C., Light Scattering by Small Particles (1957) Wiley, New York.
- [5] Tessely, B., Altmann J., and Ripperger S., Chem. Eng. Science 19 (1996), 438.
- [6] Cugniet P., PhD Dissertation, (2003), Etude de l'agrégation de particules solides en milieu non mouillant. Interprétation et modélisation, Ecole des Mines de Saint-Etienne (France).
- [7] Cournil M., Gruy F., Cugniet, P., Congrès Français de Génie des Procédés (2003), Saint-Nazaire, submitted.
- [8] Gruy, F., J. Colloid and Interf. Sci., 237 (2001), 28.
- [9] Brakalov, L.B., Chem. Eng. Sci., 42 (1987), 2373.